Thermochimica Acta, 74 (1984) 131–141
Elsevier Science Publishers B.V., Amsterdam – Printed in The Netherlands

ACID–BASE AND REDOX REACTIONS IN FUSED SODIUM NITRITE

OSAMI ABE *, TAIZO UTSUNOMIYA and YOSHIO HOSHINO

Research Laboratory of Engineering Materials, Tokyo Institute of Technology, Nagatsuta, Midori-ku, Yokohama 227 (Japan)

(Received 9 September 1983)

ABSTRACT

Acid–base and redox reactions in binary systems of sodium nitrite and several oxides with different acidity and oxidizing ability have been investigated. Kinetic parameters have been obtained by analyzing thermogravimetric data under a constant heating rate. Sodium peroxide is the main basic species in the nitrite melt. Peroxide ion is disproportionated into oxide ion and oxygen atom in the melt. The activation energy of the formation of peroxide is constant, irrespective of the acidity of oxides, while that of the disproportionation increases with increase in acidity. On the other hand, the species which possess oxidizing ability are sodium nitrite, nitrate and peroxide. The nitrate and peroxide are formed intermediately during the course of the reaction. Below 600°C, the oxidizing ability decreases in the order; peroxide, nitrite, nitrate.

INTRODUCTION

Fused alkali metal nitrates are useful as reaction media for redox processes [1–5] and as heat storage materials [6–8]. These nitrates have the advantages of low melting points, adequate surface tension and viscosity, while there are some disadvantages of relating low decomposition temperatures and high oxidizing ability. Even platinum and zirconium are known to be oxidized by nitrates [9].

Several studies have been made on the thermal decomposition of sodium nitrate [10–13] and potassium nitrate [14,15]. It is generally accepted that nitrites are formed in the first step of the thermal decomposition of nitrates. The thermal decomposition of nitrates strongly relates to the chemical properties of nitrate melts and is one of the most important problems to be solved when it is used for industrial purposes.

The thermal decomposition of sodium nitrite and the reaction of sodium nitrite with silica have been investigated previously [16]. The most important

---

* Present address: Government Industrial Research Institute, Nagoya, Hirate-cho, Kita-ku, Nagoya, 462, Japan.

0040-6031/84/$03.00

TABLE 1

List of oxide additives

Oxide additive	Specific surface area ($m^2 g^{-1}$)	Acidity ($2Z/r$ [a])
SiO_2 (Kyoritsu Yogyo Genryo Co., Ltd.)	0.2	46.9
MnO_2 (Wako Pure Chem. Ind., Ltd.)	22.3	42.9
TiO_2 (Wako Pure Chem. Ind., Ltd.)	9.2	39.6
ZrO_2 (Wako Pure Chem. Ind., Ltd.)	26.7	37.0
Al_2O_3 (Wako Pure Chem. Ind., Ltd.)	0.5	32.6
Cr_2O_3 (Wako Pure Chem. Ind., Ltd.)	2.7	30.2
MgO (Wako Pure Chem. Ind., Ltd.)	–	19.5
Na_2O	–	8.3

[a] The $2Z/r$ value increases with increase in acidity.

results obtained from the investigation are: (1) sodium nitrite has basicity (oxide ion donating ability) and oxidizing ability during its decomposition process, and (2) the basicity arises with the elapse of a constant induction period of the thermal decomposition.

Details of the acid–base and redox reactions are described in the present paper. The reactions were investigated by means of thermal analysis and the analysis of gaseous and solid reaction products. Seven oxides with different acidity and oxidizing ability were added to the nitrite.

EXPERIMENTAL

Materials

Reagent-grade sodium nitrite and nitrate from Wako Pure Chem. Ind., Ltd. were ground to below 100 mesh in an agate mortar and were dried at 200°C for 50 h. These compounds were kept in an atmosphere of argon. The acidity and surface areas of the oxide additives are listed in Table 1. Acidity is expressed as the interactive force ($2Z/r$) between oxide ion (O^{2-}) and metal cation (M^{Z+}) as

$$r = r_{11}(2Z)^{-1/(n-1)} \tag{1}$$

where r_{11} is the sum of Pauling's monovalent radii [17], Z and n are the valency of the cation and the Born exponent, respectively. The surface areas of these oxides were measured by BET method.

Apparatus and procedure

The experiments were mainly carried out by the simultaneous measurement of TG, DTA and gas chromatography. All measurements were performed in an atmosphere of argon (flow rate 50 cm^3 min^{-1}). Samples were held at 200°C for 1 h in the thermobalance to remove adsorbed water, and heated to 900°C at the rate of 5°C min^{-1}. A portion of the flow gas (1.043 cm^3) was introduced into the gas chromatograph every 2 min with an auto gas sampler and was determined quantitatively. The optimum conditions of this measurement were established from the results of previous work [10,16]. Solid reaction products were identified by X-ray diffractometry with CuK_α radiation and IR spectrometry, and were analyzed chemically.

Analytical method of thermogravimetric data

Kinetic parameters were determined by analyzing the thermogravimetric data. In general, if the temperature rises at a constant rate the reactions can be described as

$$-\frac{\mathrm{d}C}{\mathrm{d}T}=\frac{k(T)}{v}\mathrm{f}(C) \tag{2}$$

where C is the concentration of the reactant, v is the heating rate, and $k(T)$ is the kinetic constant [$k(T)=k^0\ \exp(-\Delta E/RT)$: k^0 and ΔE are the pre-exponential factor and activation energy, respectively]. Integration of eqn. (2) is given by

$$-\int\frac{\mathrm{d}C}{\mathrm{f}(C)}=\frac{k^0}{v}\int\exp\left(-\frac{\Delta E}{RT}\right)\mathrm{d}T \tag{3}$$

Integration of the right-hand side of eqn. (3) can be obtained by numerical integration [18]. Arrhenius plots, however, cannot be derived from the equation.

In the present paper, integration of the right-hand side of eqn. (3) was conducted assuming the change of $k(T)$ to be quite small in the temperature range T_0–T, and the correction factor (ϵ) to be added to ΔE to fill a gap resulted from this assumption. Then, eqn. (2) can be easily solved by

$$-\int\frac{\mathrm{d}C}{\mathrm{f}(C)}=k^0\exp\left(-\frac{\Delta E+\epsilon}{RT}\right)\frac{T-T_0}{v} \tag{4}$$

If the concentration (C) is expressed by a function of weight loss [$\mathrm{g}(\alpha)$], integration of the left-hand side of eqn. (4) is rearranged in eqn. (5)

$$S=-\int\frac{\mathrm{d}C}{\mathrm{f}(C)}=-\int\frac{\mathrm{g}'(\alpha)}{\mathrm{f}[\mathrm{g}(\alpha)]}\mathrm{d}\alpha \tag{5}$$

Equation (6) is obtained by substituting eqn. (5) into eqn. (4) and taking logarithms of both sides.

$$\ln k'=\ln k^0-\frac{\Delta E+\epsilon}{RT}=\ln S-\ln\frac{T-T_0}{v} \tag{6}$$

Kinetic parameters can be obtained from Arrhenius plots based on eqn. (6), where T_0 is the temperature at which the reaction starts, and $g(\alpha)$ is an experimental function.

RESULTS AND DISCUSSION

Reaction products

The reaction products at 700°C were sodium oxysalts (namely, metasilicate and disilicate, titanate, zirconate, and aluminate) in the systems of sodium nitrite and silica, titania, zirconia, and alumina, respectively. No reaction product was identified in the sodium nitrite and magnesia system. However, the final product in the system should be sodium oxide because the final weight loss and the kind and amount of formed gas agreed well with the equation

$$4\ NaNO_2 \rightarrow 2\ Na_2O + 4\ NO + O_2 \qquad (7)$$

Furthermore, it is noted that a relatively large amount of sodium nitrate is formed in all systems investigated here above 600°C. Sodium nitrate is known to be formed by the reaction

$$3\ NaNO_2 \rightarrow NaNO_3 + Na_2O + 2\ NO \qquad (8)$$

The reaction proceeds according to two processes [16]

$$2\ NaNO_2 \rightarrow Na_2O_2 + 2\ NO \qquad (9)$$

$$Na_2O_2 + NaNO_2 \rightarrow NaNO_3 + Na_2O \qquad (10)$$

Sodium salts such as sodium silicates and aluminate are formed by the acid–base reaction of eqn. (11)

$$2\ Na_2O_2 + x\ \text{oxide} \rightarrow 2\ Na_2O \cdot x\ \text{oxide} + O_2 \qquad (11)$$

The reactions of eqns. (10) and (11) relate to the disproportionation process of peroxide ion [eqn. (12)] in the nitrite melt [16].

$$O_2^{2-} \rightarrow O^{2-} + O \qquad (12)$$

Reaction products by the redox reaction of sodium nitrite with dichromium trioxide or manganese dioxide are described later.

Acid–base reactions in sodium nitrite melt

Figures 1 and 2 show DTA curves and the behavior of gas formation for the thermal decomposition of sodium nitrite (a,A), and the reactions of nitrite with silica (b,B), titania (c,C), zirconia (d,D), alumina (e,E) and magnesia (f,F).

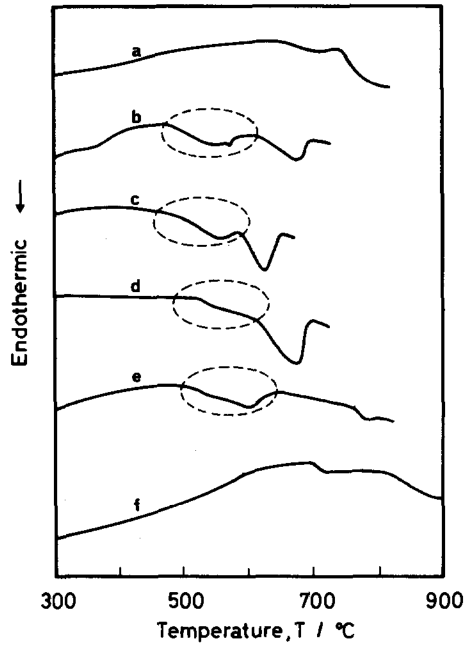

Fig. 1. DTA curves of the thermal decomposition of sodium nitrite (a) and the reactions in binary systems (b–f). a, $NaNO_2$; b, $NaNO_2 + SiO_2$ (1:2 mol); c, $NaNO_2 + TiO_2$ (1:2); d, $NaNO_2 + ZrO_2$ (1:2); e, $NaNO_2 + Al_2O_3$ (1:1); f, $NaNO_2 + MgO$ (1:2). All samples contain 13.8 mg $NaNO_2$ (0.2 mmol).

Two features are observed in the reaction of the systems containing acidic oxides. One is a relatively large amount of NO formation below 500°C (B, C and D in Fig. 2); the other is that the heat of reaction is very small. These features, however, were obscure in the system containing alumina and were not observed in the system containing magnesia (e and f in Fig. 1; E and F in Fig. 2). These facts indicate that the peroxide formed by the decomposition of nitrite [eqn. (9)] can exist stabley in the systems containing acidic oxides.

The second process of the reaction (between 500 and 600°C) is a concurrent reaction of nitrate and oxysalt formation. In this process, NO and a small amount of O_2 were formed, and endothermic peaks in DTA curves were observed (circles in Fig. 1). The temperatures at which O_2 formation can be clearly observed and the peak temperatures in DTA curves increase as the acidity of the oxide additives increases, except for the case of magnesia. Sodium salts tend to be formed at lower temperatures in the systems containing highly acidic oxides.

The final process of the reactions in these systems (above 600°C) is the reaction of sodium nitrate formed by the reaction of eqn. (10) with oxide additives. This process has been investigated previously [10].

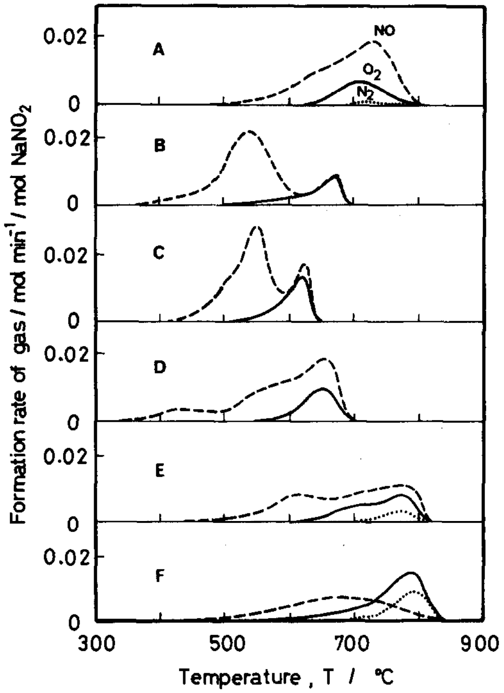

Fig. 2. Behavior of gas formation. A, $NaNO_2$; B, $NaNO_2 + SiO_2$ (1 : 2 mol); C, $NaNO_2 + TiO_2$ (1 : 2); D, $NaNO_2 + ZrO_2$ (1 : 2); E, $NaNO_2 + Al_2O_3$ (1 : 1); F, $NaNO_2 + MgO$ (1 : 2). All samples contain 13.8 mg $NaNO_2$ (0.2 mmol).

Effect of acidity of oxide additives on kinetic parameters

Figure 4 shows the Arrhenius plots obtained by analyzing the thermograms in Fig. 3 with eqn. (6), in which S is substituted by the equation

$$S = -\ln\left[\frac{2(1-1.27\alpha)}{2-1.27\alpha}\right] \tag{13}$$

Equation (13) can be derived by taking into account the stoichiometry of eqn. (10). In the plots of a, b, c, and d in Fig. 4, two kinds of linear relations are obtained corresponding to the first and second reaction process, except for the system e in which the reaction between sodium nitrite and magnesia does not occur.

The activation energy obtained from the slopes of these plots is shown in Fig. 5 as a function of the acidity of the oxide additives. The correction factor (ϵ) of 7 kJ mol^{-1} was used for the calculation of the activation energy. This value was obtained by subtracting the activation energy of an isothermal method from that of the method by eqn. (6). Values of the pre-exponential factor obtained from both methods were almost identical.

The activation energy for the first process is almost constant, irrespective of the acidity of the oxides. This fact indicates that nitrite ion has very low

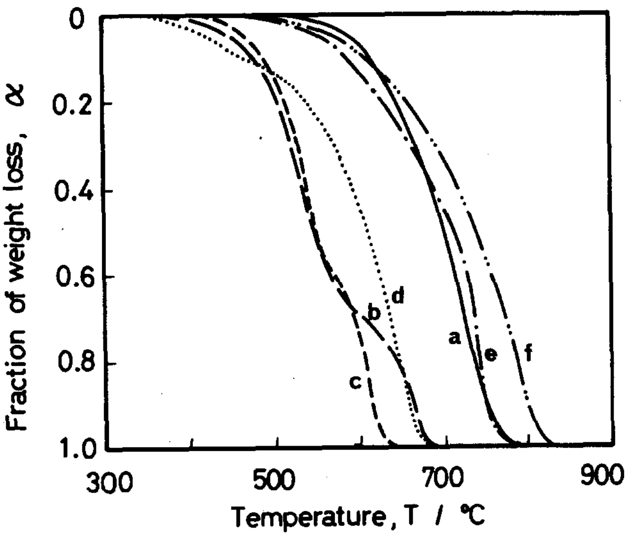

Fig. 3. TG curves for the thermal decomposition of sodium nitrite (a) and the reactions in binary systems (b–f). a, $NaNO_2$; b, $NaNO_2 + SiO_2$ (1 : 2 mol); c, $NaNO_2 + TiO_2$ (1 : 2); d, $NaNO_2 + ZrO_2$ (1 : 2); e, $NaNO_2 + Al_2O_3$ (1 : 1); f, $NaNO_2 + MgO$ (1 : 2). All samples contain 13.8 mg $NaNO_2$ (0.2 mmol).

basicity in the melt. On the other hand, the activation energy decreases with increase in the acidity of oxides in the second process. The acidity of sodium peroxide ($2Z/r = 20.6$) is higher than that of magnesia ($2Z/r = 19.5$) and lower than that of alumina ($2Z/r = 32.6$), where the acidity of sodium peroxide is estimated by using the ionic radius of 0.147 nm for peroxide ion [19]. The reaction of eqn. (10) occurs in the case of the addition of a donating oxide ion in the nitrite melt. The presence of peroxide ion as a basic species in nitrate and nitrite melts has also been reported by Al-omer and Kerridge [9] and Zambonin and Jordan [19].

Redox reactions in sodium nitrite melt

Figure 6 shows the behavior of gas formation for the reaction in binary systems of sodium nitrite and silica (A), alumina (B), manganese dioxide (C) and dichromium trioxide (D). Although manganese dioxide and dichromium trioxide have nearly the same acidity values as silica and alumina, respectively, the behavior of gas formation is quite different between the systems (A) and (C), or (B) and (D). The reactions in systems (C) and (D) have the following characteristics, comparing them with those in systems (A) and (B): (1) the amount of formed O_2 is quite small, (2) NO is formed just above the

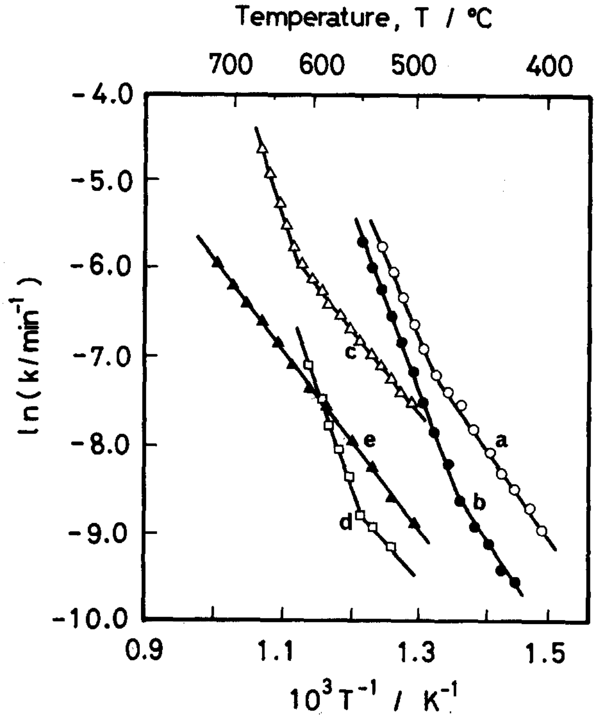

Fig. 4. Arrhenius plots using eqns. (6) and (13). a, $NaNO_2 + SiO_2$; b, $NaNO_2 + TiO_2$; c $NaNO_2 + ZrO_2$; d, $NaNO_2 + Al_2O_3$; e, $NaNO_2 + MgO$.

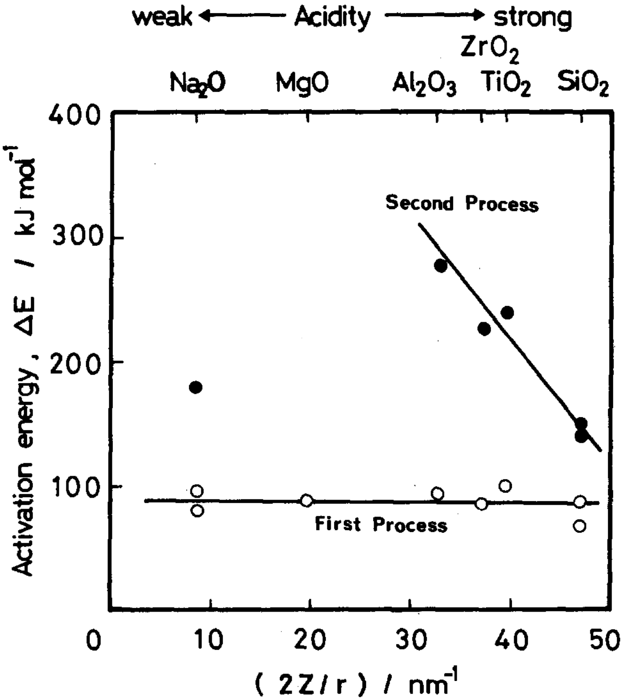

Fig. 5. Activation energy for the first and second process as a function of acidity.

melting point of sodium nitrite, and (3) the formation of N_2 and/or NO is observed below 420°C. The reduction of nitrite ion occurred at lower temperatures than in the thermal decomposition of pure nitrite. A certain amount of nitrite is reduced to N_2 in system (D), while a very small amount of nitrite is reduced in system (C) because the reducing ability of dichromium trioxide is larger than that of manganese dioxide.

In systems (C) and (D), dichromium trioxide and manganese dioxide were oxidized by sodium nitrite to form sodium chromate(VI) and manganate(V), (VI), respectively. From the observation mentioned above, the redox reaction of sodium nitrite with oxides is supposed to proceed by successive processes via some intermediates rather than a single process. This is easily explained by taking account of the ionization potential of chromium or manganese, namely, the change in the ionization potentials of Cr(III) to Cr(IV) and Mn(IV) to Mn(V) are 19 and 24 eV, respectively, while those of Cr(III) to Cr(VI) and Mn(IV) to Mn(VII) are 60 and 48 eV, respectively. The redox mechanism forming NO and N_2 can be expressed by the following reactions by assuming the presence of a series of oxide species as intermediates.

$$NO_2^- + e^- \rightarrow NO + O^{2-} \tag{14}$$

$$NO_2^- + e^- \rightarrow N + O_2^{2-} \tag{15}$$

$$O_2^{2-} + 2\,e^- \rightarrow 2\,O^{2-} \tag{16}$$

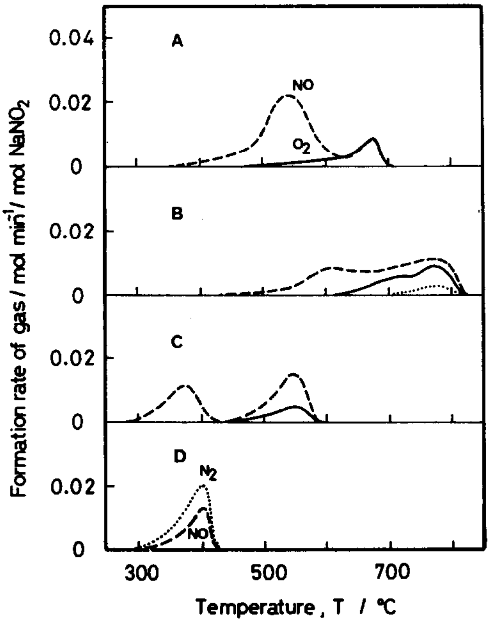

Fig. 6. Behavior of gas formation in the binary systems of sodium nitrite and silica (A), alumina (B), manganese dioxide (C) and dichromium trioxide (D). Composition: nitrite: oxide = 1 : 2 in A and C; nitrite : oxide = 1 : 1 in B and D.

$$N + N \rightarrow N_2 \tag{17}$$

The reactions of eqns. (14) and (15) are the one-electron transfer process. The peroxide ion formed by the reaction of eqn. (15) continues the oxidation process.

The formation of sodium nitrate by the decomposition of sodium nitrite is verified in system (C) above 500°C [eqn. (9)]. The behavior of gas formation in the systems containing sodium nitrate is shown in Fig. 7 for comparison with Fig. 6. The amount of formed O_2 decreases, and nitrate ion is reduced to N_2 in the systems of nitrate and manganese dioxide or chromium trioxide. Sodium nitrate also has oxidizing ability.

Sodium nitrite is oxidized by peroxide ion and forms sodium nitrate according to the reaction of eqn. (10). On the other hand, the fraction of nitrite reduced to N_2 is greater than that of nitrate in the system containing dichromium trioxide or manganese dioxide. Then, the oxidizing ability decreases in the order: peroxide, nitrite, nitrate below 600°C. The concurrent reaction of the thermal decomposition of sodium nitrate and the redox reaction occurred above 600°C.

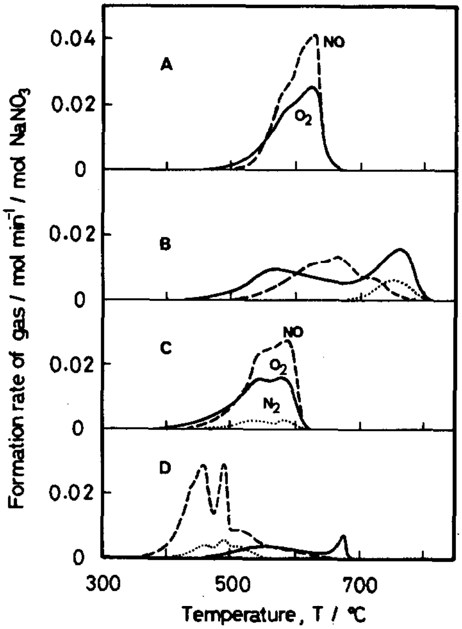

Fig. 7. Behavior of gas formation in the binary systems of sodium nitrate and silica (A), alumina (B), manganese dioxide (C) and dichromium trioxide (D). Composition, nitrate: oxide = 1 : 2 in A and C; nitrate: oxide = 1 : 1 in B and D.

REFERENCES

1 D.H. Kerridge and S.A. Tariq, Inorg. Chim. Acta, 4 (1969) 452.
2 D.H. Kerridge and S.A. Tariq, Inorg. Chim. Acta, 5 (1970) 499.
3 M. Liquornic, J. Inorg. Nucl. Chem., 33 (1971) 283.
4 B.J. Brough, D.A. Habboush and D.H. Kerridge, J. Inorg. Nucl. Chem., 30 (1972) 2870.
5 B. Morelli, E. Desimoni, L. Sabbatini and P.G. Zambonin, J. Electroanal. Chem., 94 (1978) 5.
6 C.M. Kramer and C.J. Wilson, Thermochim. Acta, 42 (1980) 253.
7 G.J. Jantz and D.J. Rogers, J. Appl. Electrochem., 13 (1983) 121.
8 G.J. Jantz and G.N. Truong, J. Chem. Eng. Data, 28 (1983) 201.
9 S.S. Al-omer and D.H. Kerridge, Inorg. Chim. Acta, 7 (1973) 665.
10 Y. Hoshino, T. Utsunomiya and O. Abe, Bull. Chem. Soc. Jpn., 54 (1981) 1385.
11 E.S. Freeman, J. Phys. Chem., 60 (1956) 1487.
12 B.D. Bond and P.W.M. Jacobs, J. Chem. Soc. A, (1956) 1265.
13 R.N. Kust and J.D. Burke, Inorg. Nucl. Chem. Lett., 6 (1970) 333.
14 E.S. Freeman, J. Am. Chem. Soc., 79 (1957) 838.
15 R.F. Bartholomew, J. Phys. Chem., 70 (1966) 3442.
16 O. Abe, T. Utsunomiya and Y. Hoshino, Bull. Chem. Soc. Jpn., 56 (1983) 428.
17 L. Pauling, The Nature of the Chemical Bond, Cornell University Press, Ithaca, 3rd edn., 1960, 514 pp.
18 N. Eisenreich, J. Therm. Anal., 19 (1980) 189.
19 P.G. Zambonin and J. Jordan, J. Am. Chem. Soc., 91 (1969) 2225.
20 T. Matsuura, Sanso Sanka Hanno, Maruzen, Tokyo, 1977, 68 pp.